Kinetics of Diffusion-Mediated DNA Hybridization in Lipid Monolayer Films Determined by Single-Molecule Fluorescence Spectroscopy

Jonas K. Hannestad,[†] Ralf Brune,[†] Ilja Czolkos,[†,⊥] Aldo Jesorka,[†] Afaf H. El-Sagheer,[‡,§] Tom Brown,[‡] Bo Albinsson,[†] and Owe Orwar[†,*]

[†]Department of Chemical and Biological Engineering, Chalmers University of Technology, 412 96, Göteborg, Sweden, [‡]School of Chemistry, University of Southampton, Highfield, Southampton, SO17 1BJ, United Kingdom, and [§]Chemistry Branch, Department of Science and Mathematics, Faculty of Petroleum and Mining Engineering, Suez Canal University, Suez, 43721, Egypt. [⊥]Present address: Department of Physics, McGill University, 3600 Rue University, H3A 2T8Montréal, QC, Canada.

ABSTRACT We use single-molecule fluorescence microscopy to monitor individual hybridization reactions between membrane-anchored DNA strands, occurring in nanofluidic lipid monolayer films deposited on Teflon AF substrates. The DNA molecules are labeled with different fluorescent dyes, which make it possible to simultaneously monitor the movements of two different molecular species, thus enabling tracking of both reactants and products. We employ lattice diffusion simulations to determine reaction probabilities upon interaction. The observed hybridization rate of the 40-mer DNA was more than 2-fold higher than that of the 20-mer DNA. Since the lateral diffusion coefficient of the two different constructs is nearly identical, the effective molecule radius determines the overall kinetics. This implies that when two DNA molecules approach each other, hydrogen bonding takes place distal from the place where the DNA is anchored to the surface. Strand closure then propagates bidirectionally through a zipper-like mechanism, eventually bringing the lipid anchors together. Comparison with hybridization rates for corresponding DNA sequences in solution reveals that hybridization rates are lower for the lipid-anchored strands and that the dependence on strand length is stronger.

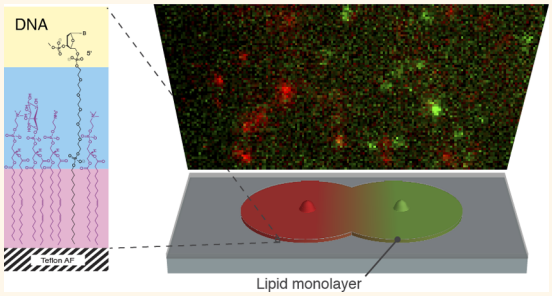

KEYWORDS: single-molecule · nanofluidics · kinetics · fluorescence · DNA · diffusion

Processes occurring in reduced dimensions such as in plasma membranes (2D) or along cytoskeletal components (1D) have an important function in biology. Examples where dimensional restrictions influence the process include G-protein assembly and function,[1] protein oligomerization,[2−4] and attachment of components in the cytoskeleton.[5,6] Molecules in systems with reduced dimensionality are restricted in mobility, and orientational order is imposed upon them. The ability to study how complex media, *e.g.*, plasma membranes, influence chemical reactions is central to our understanding of biological or biomimetic nanoscale[7] systems. To do so, it is necessary to create experimental platforms where similar restrictions such as the two-dimensional confinement of reactants in plasma membranes apply.

We have previously shown how to control chemical reactions and how to detect product formation in two-dimensional media[8] using dynamic lipid films on micropatterned substrates.[9] However, membrane-associated reactions are far from homogeneous; in contrast, natural lipid membranes are essentially mosaic,[10] and phenomena such as clustering and subdiffusion[11] influence the interaction between reacting species. Therefore, there is a need for experimental systems where individual reactions can be detected, as this would provide a more complete picture of molecular interactions between components of biological as well as artificial lipid membrane systems. Single-molecule fluorescence spectroscopy is a suitable tool to study heterogeneous processes since the detection of individual molecules and reactions avoids ensemble

* Address correspondence to orwar@chalmers.se.

Received for review August 31, 2012 and accepted December 5, 2012.

Published online December 05, 2012
10.1021/nn304010p

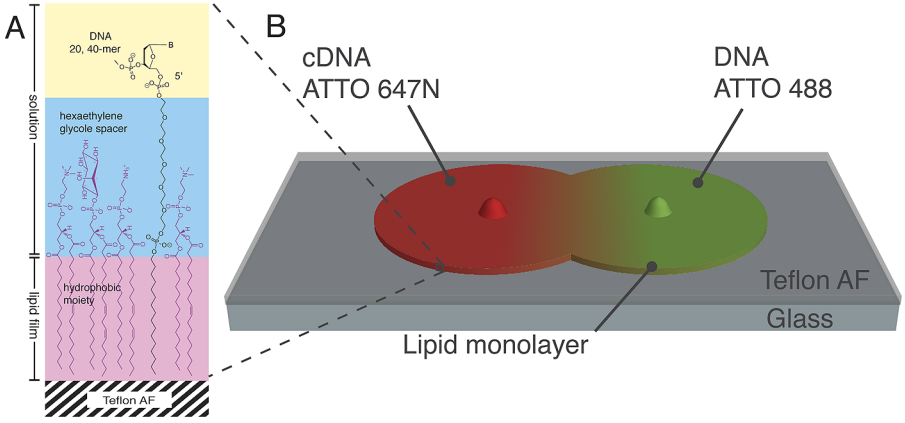

Figure 1. Lipid monolayer setup with complementary DNA strands incorporated into separate lipid sources. (A) DNA oligomer (yellow) with a spacer group (cyan) and a hydrophobic tail (magenta). The hydrophobic moiety enables incorporation of the DNA molecules into the lipid monolayer. (B) Separate multilamellar vesicles containing complementary DNA oligomers, modified at one end with a fluorophore (either ATTO 488 or ATTO 647N), are deposited onto the Teflon AF surface. As the lipid film expands, the spreading fronts meet and coalesce, and their contents mix, allowing DNA hybridization.

averaging typical for bulk measurements and enables the detection of rare events.

In order to extract kinetic information from systems of small scale or reduced dimensionality, detection of individual reaction events is highly beneficial. For instance, Chan *et al*. detected docking of bilayer-anchored vesicles,[12] and Rocha *et al*. investigated the activity of single lipase molecules in lipid bilayers.[13]

Here, we use single-molecule fluorescence spectroscopy to monitor individual reactions occurring in nanofluidic lipid monolayer films. We have chosen to work with membrane-anchored complementary DNA molecules, which are allowed to diffuse and to hybridize while associated to the two-dimensional lipid monolayer film. To allow the incorporation of DNA into the lipid monolayer film, the two DNA strands have a hydrophobic moiety at either the 3′ or the 5′ end. The length of the hydrophobic anchor approximately matches the thickness of the hydrophobic part of a lipid monolayer (shown in magenta in Figure 1A). A spacer group (cyan part in Figure 1A) increases the interaction radius as well as the flexibility and orientational freedom of the DNA molecule. To be able to study the influence of strand length on the reaction rate, we use two sets of complementary strands, one 20-mer (DNA1, cDNA1) and one 40-mer (DNA2, cDNA2) (Table 1). The single-stranded DNAs are labeled with either ATTO 488 (DNA1, DNA2) or ATTO 647N (cDNA1, cDNA2) to allow the simultaneous detection of both.

In order to link the observed interactions to a measure of reaction probability, we performed lattice diffusion simulations. This enables us to both map individual reactions on the single-molecule level and determine an overall reaction rate for the system.

Figure 1B shows the DNA-containing multilamellar vesicles deposited on the Teflon AF surface. Once the vesicles are placed on the Teflon AF surface, the lipid film starts to spread, shielding the hydrophobic surface from the surrounding aqueous solution. As the spreading fronts meet, the DNA payload molecules can mix. Mixing of complementary DNA strands then allows for the formation of duplex DNA. To ascertain that the DNA molecules are moving due to diffusion only, the lipid monolayers were allowed to spread extensively. This way, it is assured that the lipid monolayer in between the vesicles, where measurements are performed, is dense and does not flow due to tension gradients.

TABLE 1. List of Oligonucleiotides Used

descriptor	3′ modification	5′ modification	sequence (5′ to 3′)
DNA1	ATTO 488	C16-HEG	TCAGTGATTAGTCATGCAGA
cDNA1	C16-HEG	ATTO 647N	TCTGCATGACTAATCACTGA
DNA2	ATTO 488	C16-HEG	TCAGTGATTAGTCATCTCGTATTC-TTGCTATCTCGATATT
cDNA2	C16-HEG	ATTO 647N	AATATCGAGATAGCAAGAATACGA-GATGACTAATCACTGA

RESULTS AND DISCUSSION

Previously used substrate materials for lipid monolayer spreading are for instance the epoxy photoresists SU-8 and EPON 1002F.[8] Unlike SU-8 or EPON 1002F, Teflon AF is virtually nonfluorescent. Teflon AF is therefore the substrate material of choice since minimization of background fluorescence is imperative for single-molecule fluorescence detection. Teflon AF also has a low refractive index, which is advantageous for optical applications. Moreover, Czolkos *et al*. have found that lipid monolayer spreading and lateral diffusion of lipids are significantly faster compared to the previously used epoxy photoresist substrates.[14] These accelerated dynamics are attributed to the lower sliding friction that lipid molecules experience in contact with Teflon AF compared to SU-8 or EPON.

By simultaneous excitation of the two dyes, it is possible to follow the two complementary strands as

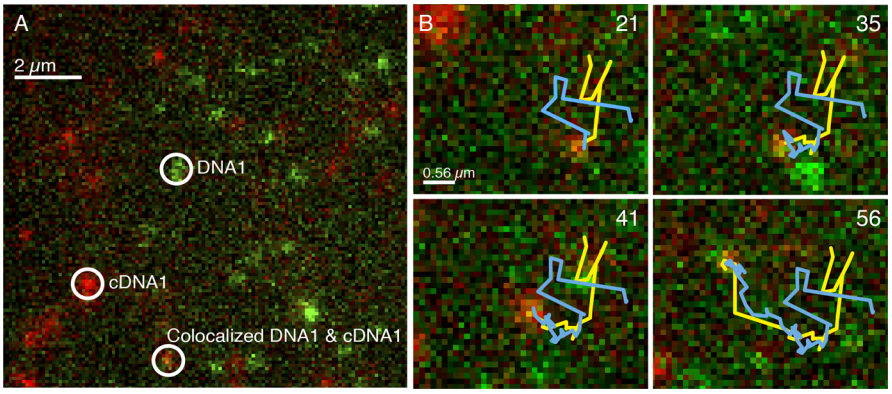

Figure 2. Single-molecule tracking of diffusing DNA molecules at 1:150 000 DNA:lipid ratio. (A) Fluorescence micrograph of a lipid monolayer decorated with the 20-mer DNA molecules DNA1 (green) and cDNA1 (red) on a Teflon AF surface. Co-localized DNA1 and cDNA1 appear as yellow pixels. The image is false-colored red and green, and the two channels have been overlaid. (B) Time series from the same experiment as in (A) of two diffusing complementary DNA molecules, DNA1 (green) and cDNA1 (red), recorded at 30 ms/frame. The numbers indicate the current 30 ms time frame. The trajectories of both DNA1 and cDNA1 are visualized with blue and yellow lines, respectively, showing the migrated path up to the depicted time frame. After the two strands have met in frame 21, they show coupled motion, indicating hybridization. The coupled motion is retained until the fluorophores photobleach.

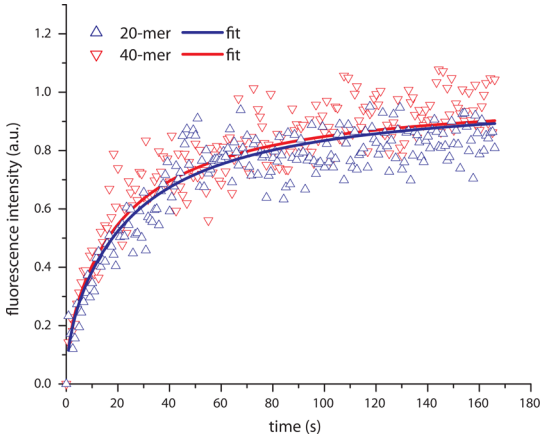

Figure 3. Measured fluorescence recovery after photobleaching and fitted recovery curve for 20-mer (blue) and 40-mer C16-HEG-DNA in lipid monolayer film spreading on Teflon AF. DNA:lipid ratio is 1:150.

they mix and hybridize. Figure 2A shows a sampled image of two complementary 20-mer DNA strands mixed in the lipid monolayer film. Figure 2B shows how two of the strands meet (frame 21) and then hybridize, forming double-stranded DNA. The reaction is verified by the positional correlation between the strand movements in the frames following the docking event (frames 35, 41, and 56 are presented as examples in Figure 2B). To ensure that co-migration is due to duplex formation and not just a chance effect or random walk, the two strands have to follow each other long enough for co-migration through independent diffusion to be improbable. How far the two strands have to move together depends on their rate of diffusion. Using fluorescence recovery after photobleaching (FRAP) we determined the average diffusion coefficient for monolayer-anchored DNA molecules to be $D = 0.8\ \mu m^2/s$ for both the 20-mer and 40-mer DNA (Figure 3). The same average diffusion coefficient was obtained from the displacement of individual diffusers between two adjacent time frames using the same method as Rocha *et al.*[13] From the diffusion coefficient, the root-mean-square displacement of the individual DNA strands during 90 ms (3 × 30 ms frame rate) was calculated to be 0.54 μm. On the basis of statistical diffusion in two dimensions we obtain a probability that two independent diffusers would randomly migrate such a distance together to be approximately 0.01. From this, we determine that for a pair of co-localized complementary strands to be considered as possible duplexes they must co-migrate for at least three consecutive time frames. Instances where the two strands initially co-migrated but then continued to move independently were not counted as successful hybridization events. The event shown in Figure 2 confirms that there is duplex formation occurring between the complementary strands incorporated in the lipid monolayer film. A movie showing the sequence depicted in Figure 2 is available in the online Supporting Information (S2).

Reactions occurring between membrane-localized components are governed by a large number of factors. First, the reactants must diffuse across the surface to be able to interact. A particle diffusing in two dimensions has a probability of unity to return to its initial position.[15,16] This means that mixing by diffusion is not ideal in two dimensions. When mixing of components is driven by diffusion, the frequency of collisions between reactants will strongly depend on their diffusivity. A low diffusion coefficient combined with a low reactant density entails that collision events are comparatively rare. Second, when the reactants, in this case complementary DNA strands, come close enough to interact with each other, they must in addition assume the correct orientation. In a system where there is a high degree of flexibility, the number of possible orientations is large. Here, restraint is imposed on the reactants due to the

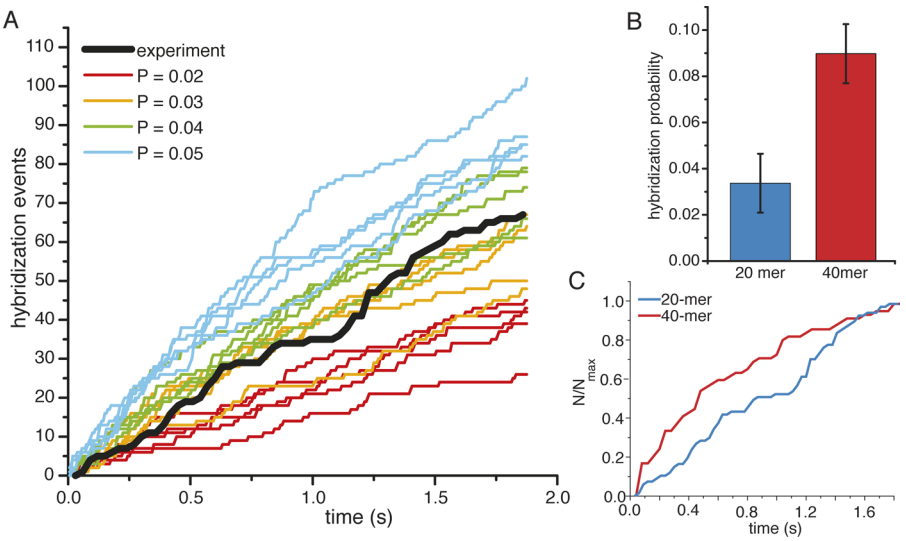

Figure 4. Detected hybridization events compared to results from lattice diffusion simulations. (A) By applying lattice diffusion calculations to distributions obtained from the fluorescence measurements of the two complementary DNA molecules it is possible to simulate possible outcomes from different scenarios. When the two complementary strands occupy the same grid point at the same time, they have the chance to hybridize, which is governed by the hybridization probability *P*. The figure shows experimental results for the hybridization of the 20-mer DNA1 with cDNA1 (black) as well as simulated outcomes for different set values of *P*. Curves that have the same color have identical input variables. Any difference is therefore purely stochastic. From the graph, it can be seen that the $P = 0.03$ to $P = 0.04$ traces correspond best to the results of our measurements. (B) Average reaction probabilities (*P*) from three separate samples for each of the two different strand combinations. The *P* values are calculated from least-squares fits of experimental data to lattice diffusion simulations similar to those shown in (A). Error bars represent the standard deviation. The results show average *P* values of 0.034 and 0.091 for the 20-mer and the 40-mer, respectively. (C) Two normalized accumulations of hybridization events for complementary 20-mer (blue) and 40-mer (red) DNA. The shape of the curve varies between experiments and depends on the distribution of the complementary DNA strands in the experiment.

surface attachment, providing a larger degree of orientational order. However, due to the flexible hexaethylene glycol spacer, the DNA moiety still has substantial freedom to probe its surrounding. In addition, the complementary DNA molecules must search the sequences to find sufficient overlap so that the formed duplex is stronger than the diffusive movement dragging the two strands apart.

To investigate the probability with which two strands could encounter each other and subsequently form a duplex, we performed lattice diffusion simulations based on strand distributions in a fully mixed system. As input, we used strand positions obtained from actual experiments. The mesh size for the simulation was the same as the pixel size in the experimental images, 0.1 μm $\times$ 0.1 μm, and the step-time was set so that a diffusing molecule moves one square in each time frame. To determine the step length, the diffusion coefficient of single-stranded C16-HEG-DNA in a lipid monolayer was used. This was measured with FRAP to be 0.8 $\mu m^2/s$ for both the 20-mer and the 40-mer. When two complementary strands simultaneously occupy the same grid point, they have the possibility to hybridize. By using the hybridization probability as a variable, we determined the reaction rate in a simulation. Figure 4A shows an accumulation of detected hybridization events as lipid films containing complementary DNA strands (DNA1 and cDNA1) are allowed to mix. This is compared with simulated outcomes for different sets of reaction probabilities, *P*. The reaction probability, *P*, was estimated by least-squares fitting of the experimental data to simulation outcomes for four different probability values (0.02, 0.03, 0.04, and 0.05 for the 20-mer, 0.08, 0.09, 0.1, and 0.11 for the 40-mer) and with five simulations at each value. The comparison between the experimental results using 20-mer DNA with those from the simulations reveals average matching rates for $P = 0.034$. For the 40-mer DNA (DNA2 and cDNA2), the average reaction probability is 0.091, as shown in Figure 4B. The difference in reaction rate for different strand lengths shows that the overall rate is not alone dictated by diffusion but also by the affinity between the two reactants. Therefore, an explanation involving both general mechanisms for duplex formation and system-specific properties such as surface orientation and lateral diffusion of the DNA molecules is needed.

When two complementary DNA strands come close enough to form hydrogen bonds, there is an initial phase when the first base pair is being formed. At this stage, the newly formed duplex can open and close repeatedly. As the second base pair is formed, the connection strength between the complementary strands increases and the formation of the complete duplex in a zipper-like fashion is facilitated.[17] The time scale for the formation of the second base pair is on the order of 0.5−1 ns.[17] During this time, very little lateral movement of the individual strands occurs. On the way from the initial base pairs to the final duplex, the strand has to

go through a number of semistable stages before the correct base pairing pattern is found. These intermediates help to keep the strands from diffusing out of base pairing distance. With longer strand length, the number of possible stable intermediates holding the two strands together is higher, resulting in a higher probability for the duplex to form. This increased stability is reflected in the increase in melting temperature with increasing strand length. In an aqueous bulk solution, the 20-mer and 40-mer DNA strands used in the experiments have melting temperatures of approximately 57 and 68 °C, respectively. Thus, at room temperature the likeliness that two hybridized strands dissociate is low. A higher probability for a stable duplex to form leads to a higher reaction rate at the ensemble level. Furthermore, when the reaction probability is low, *i.e.*, when the number of co-localizations is much larger than the number of reaction events, the stochastic nature of diffusion will have an additional strong influence on the behavior of the system. In Figure 4A, this is indicated by the wide range of simulation outcomes despite identical starting configurations and reaction probabilities. Because the overall reaction probability is relatively low, both for the 20-mer and the 40-mer, small differences in reaction probability can result in large differences in the outcome of the reaction. In biology, stochastic events play an important role in cellular functions, such as gene regulation[18,19] or Ca^{2+} signaling.[20] It is therefore important to create experimental models where such processes can be controlled and studied.

Previous work on DNA hybridization kinetics showed that reaction rates to a large extent depend on the environment where the reaction takes place,[21,22] but also the presence of secondary structure influences the rate of the reaction.[22−25] In general, DNA hybridization in bulk solution proceeds as a second-order reaction, with the two complementary strands as the two reactants.[25] However, reactions occurring between components confined to two dimensions do not behave in the same way as in three dimensions. For reactions in 2D, rate constants are not invariant with time; instead rates decrease as a power law of reaction time: $k \propto t^{-h}$, where h is a constant and $0 \leq h \leq 1$.[26] This gives rise to reaction orders that have fractal dimensionality. For the two different DNA strand lengths that we have investigated, the reactions proceed somewhat differently. Figure 4C shows examples of accumulation of formed duplexes over time, both for the 20-mer and for the 40-mer DNA. The number of formed duplexes increases in a linear fashion for the 20-mer, while, in the case of the 40-mer, the rate of increase has a stronger tendency to level off with time. The reaction rate in a diffusion-controlled reaction depends on the collision frequency of the two reacting species, in this case, complementary DNA strands. Therefore, if the collision frequency varies over time, the reaction rate will also vary.[16] For reactants diffusing in a two-dimensional medium, the molecules primarily experience and probe their local environment (*vide supra*). This means that local heterogeneities in reactant concentrations can result in localized variations in collision frequencies, as there is little long-range mixing of the system. When two complementary DNA strands hybridize and form a duplex, a transiently localized decrease in the concentration of single-stranded DNA is the result. If the probability for this is sufficiently high, the diffusional mixing will not be sufficient, and this will have an effect on the system as a whole. It is therefore possible to observe a decreasing reaction rate although the number of unreacted species is plentiful. The observed decrease in reaction rate constant in certain 40-mer samples might be attributed to such an effect, as the probability to form a duplex upon collision is higher for the 40-mer than for the 20-mer.

By comparing the reaction rates obtained from our experiments with DNA hybridization kinetics measured in solution, we obtain an estimate on how the transfer from a three-dimensional solution to a two-dimensional lipid film affects the hybridization rate. In solution, the corresponding strands result in hybridization rates of 2.7×10^5 and 4.0×10^5 M^{-1} s^{-1} for the 20-mer and 40-mer, respectively (see Supporting Information). Comparing solution kinetics with surface kinetics is not straightforward. However, using the duplex formation rate at the surface together with the DNA density at the surface, and assuming a solution with molecular density, we can, using a second-order reaction model, calculate approximate corresponding solution rates to be 0.7×10^5 and 1.4×10^5 M^{-1} s^{-1} for the surface-associated 20-mer and 40-mer DNA strands, respectively (a more detailed description of the conversion from a 2D molecular density to a 3D concentration value is provided in the Supporting Information).

Besides the probability to form a stable duplex, strand length affects the reactivity in a different way. When two complementary single DNA strands are in close proximity, they must probe their local environment to obtain an orientation that enables duplex formation. The C16-HEG-DNA construct allows for bending and rotational freedom that gives the protruding DNA strands an approximately hemispherical volume, which can be probed for interaction partners. The exact shape of this volume depends on the interactions between the DNA strand and the lipid layer as well as the rigidity of the DNA and linker moieties. However, the volume is naturally larger for a longer strand than for a shorter one. A schematic image showing the difference in probed volume for the two different strand lengths is provided in Figure 5A. Results from molecular dynamics simulations on tethered DNA molecules show extensive bending of the DNA molecule on the time scale of tens of nanoseconds, both with respect to the surface and in the backbone of the DNA molecule itself.[27,28]

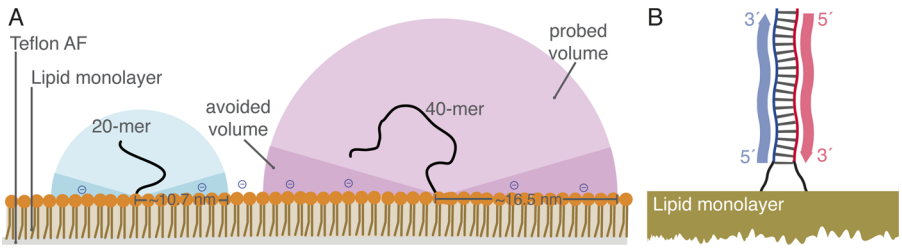

Figure 5. Schematics of C16-HEG-DNA in lipid film. (A) Schematic showing the probed hemispherical volume for a 20-mer (left) and a 40-mer (right) C16-HEG-DNA when incorporated into a lipid monolayer. The size of the probed volume corresponds to fully extended single-stranded DNA. A small part of the hemisphere close to the lipid surface is avoided by the DNA (darker regions), primarily due to electrostatic repulsion from the predominantly negatively charged lipid layer. (B) The antiparallel orientation of the tethered complementary strands facilitates duplex formation.

Reactions occurring in two-dimensional space proceed in different ways than reactions occurring in three dimensions. In two-dimensional systems such as lipid monolayers, molecules have orientational order, whereas in three-dimensional bulk systems, orientational disorder prevails. For the case of C16-HEG-DNA molecules anchored to lipid monolayers, this means that all DNA molecules are in the first place aligned perpendicular to the substrate, considering the central axis of the hemispherical volume that they can probe. Furthermore, the DNA sequences were designed to be antiparallel (Figure 5B). This order increases the probability for reactions since molecular motion is restricted in a way that favors successful interactions. However, content mixing by diffusion is less efficient in two dimensions than in three dimensions. On one hand, this means that it takes longer for two separate reactants to find each other. On the other hand, it also means that two reactants that are close together will remain so for a longer time, increasing the probability for reaction to occur.

To summarize, the probability for two DNA strands undergoing two-dimensional diffusion to hybridize depends on the collision frequency, the interstrand orientation, the overlap volume, and the occupation time in the reactive radius. The reaction probability can be modeled as a product of the mentioned factors, as expressed in eq 1

$$P \propto f_c b V \tau \qquad (1)$$

where f_c is the collision frequency for the two complementary C16-HEG-DNA strands in the lipid film, b the orientation factor, V the overlap volume, and τ the time that two complementary strands that have collided stay within the area in which they can interact. Both the collision frequency and the occupation time depend on the lateral diffusion rate, while the interstrand orientation depends on the chain dynamics of the DNA strands forming the duplex. The occupation time and the overlap volume are both dependent on the strand length of the DNA moiety. Because the DNA strands move by diffusion, the occupation time will be directly related to the size of the part of the molecule that protrudes into the solution (linker and DNA moieties). The diffusing single-stranded DNA molecules assume a random coil conformation with a radius, R, proportional to $L^{0.5}$, where L is the number of units in the polymer (DNA) chain. From the hydrodynamic radius of the DNA moiety and the diffusive motion of the molecule in the lipid film we derive $\tau \propto L$. The orientation factor b can be assumed to be a constant ranging from 0 to 1, with 0 and 1 representing completely antiparallel and completely parallel strands, respectively. The overlap volume, V, is the average volume where interaction between the two complementary strands is possible. This can be modeled as two intersecting hemispheres, each with the radius R. The time-averaged overlap volume is given in eq 2:

$$V \approx \frac{1}{\tau}\int_0^{\tau} \frac{\pi}{24}(4R + \mathrm{d}(t))(2R - \mathrm{d}(t))^2 \mathrm{d}t \qquad (2)$$

where d is the distance between the anchoring points of the two complementary DNA strands. In eq 2 we assume that the DNA strands access a hemispherical volume. However, as stated above, there is an avoided volume close to the lipid layer due to electrostatic repulsion that is not accounted for in the equation. As the DNA strands of different length do not differ in their lateral mobility, the collision frequency cannot account for the observed difference in reaction probability. Instead, it is the difference in volume that the protruding DNA strand occupies that most likely dictates the likelihood of hybridization as two complementary strands come in contact with each other.

CONCLUSIONS

In this paper, we have shown how reactions occurring between components associated to lipid monolayer films can be monitored using single-molecule fluorescence spectroscopy. Our results show that there is a significant dependence of the reaction rate on DNA strand length, *i.e.*, affinity. Additionally, we have observed substantial heterogeneity in the movement of the membrane-incorporated molecules present in our experiments. The exact nature of the observed heterogeneity is unclear and warrants further investigation. A detailed understanding of heterogeneous processes in complex media would provide valuable insight into many biochemical processes.

The combination of positional and orientational order and control offered by the transition from three to two dimensions together with the ability to detect single reaction events constitutes a powerful tool for nanoscale assembly. By combining these parameters with flow control, a single device could be developed to simultaneously handle single-molecule synthesis, assembly of supramolecular structures,[29] and detection of individual reactions. These functions can then easily be parallelized in small scale by micro- and nanofabrication.

The ability to follow diffusion and reactions of individual molecules in a fluid two-dimensional medium is of great importance for the understanding of membrane-localized processes whose heterogeneous nature is difficult to study. The techniques presented in this paper can provide new insight for combining both reaction control and detection of rare events.

MATERIALS AND METHODS

Lipid Preparation. Lipids were prepared as described by Karlsson *et al.*[30] In short, the lipid solutions (soybean polar extract (SPE) (Avanti Polar Lipids)) were spiked with molecule DNA1, cDNA1, DNA2, or cDNA2 (see Table 1) at a DNA:lipid molar ratio of 1:150 000 and equilibrated at 8 °C for at least 10 h for the DNA to incorporate into the lipid layer. A 2 μL amount of the equilibrated DNA–lipid mixture was dried under reduced pressure for at least 40 min and rehydrated with PBS buffer (5 mM TRIZMA base, 30 mM K_3PO_4 (both Sigma), 30 mM KH_2PO_4, 1 mM $MgSO_4$ (both Merck), and 0.5 mM EDTA (Fluka) adjusted with KOH (Sigma) to pH 7.8) for approximately 10 min. Deionized water was taken from a Milli-Q system (Millipore).

Substrate Preparation. Microscope coverslides from Menzel Gläser (Braunschweig, Germany) were thoroughly cleaned (megasonication in water, blow-dried in a nitrogen stream, 2 min at 250 W in a 300PC Plasma Strip (PVA TePla AG, Germany)). Teflon AF solution (601S1-100-6, 6% (w/w) solids, DuPont, Wilmington, DE, USA) was diluted with Fluorinert FC-77 (CAS: 86508-42-1, Larodan, Malmö, Sweden) to contain 1.2% (w/w) solids. This solution was spin-coated (2000 min^{-1}, 1 min) onto the glass coverslides. The coverslides were baked at 180 °C for 5 min to surpass Teflon AF's glass transition temperature and were allowed to cool below 55 °C before they were removed from the hot plate.

Fluorescence Microscopy. The 488 nm laser line of an Ar-ion laser (Sabilite, SpectraPhysics) is combined with a 641 nm laser line (Cube, Coherent). Wide-field illumination of the sample is obtained by focusing an expanded beam at the back focal plane of the microscope objective (Leica DM IRB equipped with a 100× 1.40 NA objective). Emitted light was collected through the objective and split into two spectrally separate components corresponding to the two used dyes using an Optosplit II (Cairn Research). The two emission channels were recorded on one EM-CCD (DV887, Andor). The microscopy setup is schematically depicted in Figure S1 in the Supporting Information. The recorded images were false colored and overlaid using Andor IQ. The trajectories of the single diffusing molecules were traced using Andor Tracker. Spots that were immobile and at least two times brighter than the average spot were treated as aggregates and were not tracked.

Lattice Diffusion Simulations. Initial particle positions were obtained from experiments using Andor IQ Tracker software. The lattice size was 0.1 μm × 0.1 μm, and the time step was determined from the characteristic diffusion of the C16-HEG-DNA in the lipid monolayer to be 6.5 ms. Periodic boundary conditions were used at all edges since the simulation portrays the conditions in a small patch in the middle of the lipid monolayer. The two species are allowed to move independently in the modeled area. If two complementary strands occupy the same lattice square at the same time, they have the chance to form a duplex. This process is governed by the reaction probability, which is a free parameter. If the strands hybridize, they are removed from the simulation. The cumulative number of detected hybridization events is recorded.

Determination of Diffusion Coefficients through Fluorescence Recovery after Photobleaching. Bulk diffusion coefficients of the single-stranded C16-HEG-DNA molecules Teflon AF were determined using fluorescence recovery after photobleaching. For these measurements molecules cDNA1 (20-mer) and cDNA2 in SPE lipids were used at 1:150 DNA–lipid concentration ratio. For the FRAP measurements a Leica IRE2 confocal microscope equipped with a Leica TCS SP2 confocal scanner was used. The ATTO 647N dye used to label the DNA molecules was excited using the 633 nm laser line of the confocal setup, and fluorescence was recorded in the 650–800 nm range. After the lipid material had spread to form a homogeneous monolayer, a circular patch (diameter 7.5 μm) of the film was exposed to intense laser radiation to bleach the fluorescent dyes. Following this, the recovery of the fluorescence intensity was recorded. The recovery data were then fitted to a modified Bessel function and the "characteristic" diffusion time, τ_D, was estimated.

Conflict of Interest: The authors declare no competing financial interest.

Acknowledgment. This work was made possible through financial support obtained from the European Research Council (ERC Advanced Grant), The Swedish Research Council (VR), and the Knut and Alice Wallenberg Foundation. A.H.E.-S. and T.B. have received funding from the European Community 7th Framework Programme [FP7/2007-2013], grant agreement [HEALTH-F4-2008-201418] entitled READNA. I.C.'s work was funded by the Swedish Government NanoInitiative.

Supporting Information Available: S1. Supporting Information covering oligonucleotide synthesis, bulk hybridization kinetics measurements, and conversion from 2D surface density to 3D concentration. S2. Movie showing the co-migration of two hybridized DNA strands. This material is available free of charge *via* the Internet at http://pubs.acs.org.

REFERENCES AND NOTES

1. Gilman, A. G. G-Proteins–Transducers of Receptor-Generated Signals. *Annu. Rev. Biochem.* **1987**, *56*, 615–649.
2. Štefanová, I.; Hořejši, V.; Ansotegui, I. J.; Knapp, W.; Stockinger, H. GPI-Anchored Cell-Surface Molecules Complexed to Protein Tyrosine Kinases. *Science* **1991**, *254*, 1016–1019.
3. Rath, A.; Deber, C. A. Surface Recognition Elements of Membrane Protein Oligomerization. *Proteins* **2008**, *70*, 786–793.
4. Rath, A.; Deber, C. M. Membrane Protein Assembly Patterns Reflect Selection for Non-Proliferative Structures. *FEBS Lett.* **2007**, *581*, 1335–1341.
5. Voeltz, G. K.; Prinz, W. A. Sheets, Ribbons and Tubules: How Organelles Get Their Shape. *Nat. Rev. Mol. Cell Biol.* **2007**, *8*, 258–264.
6. Egea, G.; Lázaro-Diéguez, F.; Vilella, M. Actin Dynamics at the Golgi Complex in Mammalian Cells. *Curr. Opin. Cell Biol.* **2006**, *18*, 168–178.
7. Karlsson, M.; Davidson, M.; Karlsson, R.; Karlsson, A.; Bergenholtz, J.; Konkoli, Z.; Jesorka, A.; Lobovkina, T.; Hurtig, J.; Voinova, M.; *et al*. Biomimetic Nanoscale Reactors and Networks. *Annu. Rev. Phys. Chem.* **2004**, *55*, 613–649.
8. Czolkos, I.; Hannestad, J. K.; Jesorka, A.; Kumar, R.; Brown, T.; Albinsson, B.; Orwar, O. Platform for Controlled Supramolecular Nanoassembly. *Nano Lett.* **2009**, *9*, 2482–2486.

9. Czolkos, I.; Erkan, Y.; Dommersnes, P.; Jesorka, A.; Orwar, O. Controlled Formation and Mixing of Two-Dimensional Fluids. *Nano Lett.* **2007**, *7*, 1980–1984.
10. Simons, K.; Ikonen, E. Functional Rafts in Cell Membranes. *Nature* **1997**, *387*, 569–572.
11. Nicolau, D. V.; Hancock, J. F.; Burrage, K. Sources of Anomalous Diffusion on Cell Membranes: A Monte Carlo Study. *Biophys. J* . **2007**, *92*, 1975–1987.
12. Chan, Y. H. M.; Lenz, P.; Boxer, S. G. Kinetics of DNA-Mediated Docking Reactions between Vesicles Tethered to Supported Lipid Bilayers. *Proc. Natl. Acad. Sci. U. S. A.* **2007**, *104*, 18913–18918.
13. Rocha, S.; Hutchison, J. A.; Peneva, K.; Herrmann, A.; Muellen, K.; Skjot, M.; Jorgensen, C. I.; Svendsen, A.; De Schryver, F. C.; Hofkens, J.; *et al*. Linking Phospholipase Mobility to Activity by Single-Molecule Wide-Field Microscopy. *ChemPhysChem* **2009**, *10*, 151–161.
14. Czolkos, I.; Guan, J.; Orwar, O.; Jesorka, A. Flow Control of Thermotropic Lipid Monolayers. *Soft Matter* **2011**, *7*, 6926–6933.
15. de Gennes, P. G. Kinetics of Diffusion-Controlled Processes in Dense Polymer Systems 0.1. Non-Entangled Regimes. *J. Chem. Phys.* **1982**, *76*, 3316–3321.
16. Berry, H. Monte Carlo Simulations of Enzyme Reactions in Two Dimensions: Fractal Kinetics and Spatial Segregation. *Biophys. J.* **2002**, *83*, 1891–1901.
17. Monti, S.; Cacelli, I.; Ferretti, A.; Prampolini, G.; Barone, V. Simulating DNA Hybridization on an Amine-Functionalized Silicon Substrate. *J. Phys. Chem. B* **2010**, *114*, 8341–8349.
18. Elowitz, M. B.; Levine, A. J.; Siggia, E. D.; Swain, P. S. Stochastic Gene Expression in a Single Cell. *Science* **2002**, *297*, 1183–1186.
19. Rosenfeld, N.; Young, J. W.; Alon, U.; Swain, P. S.; Elowitz, M. B. Gene Regulation at the Single-Cell Level. *Science* **2005**, *307*, 1962–1965.
20. Wang, S.-Q.; Song, L.-S.; Lakatta, E. G.; Cheng, H. Ca^{2+} Signalling between Single L-Type Ca^{2+} Channels and Ryanodine Receptors in Heart Cells. *Nature* **2001**, *410*, 592–596.
21. Schoen, I.; Krammer, H.; Braun, D. Hybridization Kinetics Is Different inside Cells. *Proc. Natl. Acad. Sci. U. S. A.* **2009**, *106*, 21649–21654.
22. Sekar, M. M. A.; Bloch, W.; St John, P. M. Comparative Study of Sequence-Dependent Hybridization Kinetics in Solution and on Microspheres. *Nucleic Acids Res.* **2005**, *33*, 366–375.
23. Gao, Y.; Wolf, L. K.; Georgiadis, R. M. Secondary Structure Effects on DNA Hybridization Kinetics: A Solution *versus* Surface Comparison. *Nucleic Acids Res.* **2006**, *34*, 3370–3377.
24. Schwille, P.; Oehlenschläger, F.; Walter, N. G. Quantitative Hybridization Kinetics of DNA Probes to RNA in Solution Followed by Diffusional Fluorescence Correlation Analysis. *Biochemistry* **1996**, *35*, 10182–10193.
25. Parkhurst, K. M.; Parkhurst, L. J. Kinetic Studies by Fluorescence Resonance Energy Transfer Employing a Double-Labeled Oligonucleotide: Hybridization to the Oligonucleotide Complement and to Single-Stranded DNA. *Biochemistry* **1995**, *34*, 285–292.
26. Kopelman, R. Rate Processes on Fractals: Theory, Simulations, and Experiments. *J. Stat. Phys.* **1986**, *42*, 185–200.
27. Wong, K. Y.; Pettitt, B. M. Orientation of DNA on a Surface from Simulation. *Biopolymers* **2004**, *73*, 570–578.
28. Barone, V.; Cacelli, I.; Ferretti, A.; Monti, S.; Prampolini, G. Sensors for DNA Detection: Theoretical Investigation of the Conformational Properties of Immobilized Single-Strand DNA. *Phys. Chem. Chem. Phys.* **2009**, *11*, 10644–10656.
29. Gu, H. Z.; Chao, J.; Xiao, S. J.; Seeman, N. C. A Proximity-Based Programmable DNA Nanoscale Assembly Line. *Nature* **2010**, *465*, 202–206.
30. Karlsson, M.; Nolkrantz, K.; Davidson, M. J.; Strömberg, A.; Ryttsen, F.; Åkerman, B.; Orwar, O. Electroinjection of Colloid Particles and Biopolymers into Single Unilamellar Liposomes and Cells for Bioanalytical Applications. *Anal. Chem.* **2000**, *72*, 5857–5862.